NUCL SCI TECH (2018) 29:104
https://doi.org/10.1007/s41365-018-0431-z

Gamma irradiation-induced effects on the properties of TiO_2 on fluorine-doped tin oxide prepared by atomic layer deposition

Syed Mansoor Ali[1] · M. S. Algarawi[1] · Turki S. ALKhuraiji[2] · S. S. Alghamdi[1] · Muhammad Hammad Aziz[3] · M. Isa[4]

Received: 13 April 2017 / Revised: 7 November 2017 / Accepted: 14 December 2017 / Published online: 30 May 2018

Abstract The effect of gamma irradiation with different doses (25–75 kGy) on TiO_2 thin films deposited by atomic layer deposition has been studied and characterized by X-ray diffraction (XRD), photoluminescence measurements, ultraviolet–visible (UV–Vis) spectroscopy, and impedance measurements. The XRD results for the TiO_2 films indicate an enhancement of crystallization after irradiation, which can be clearly observed from the increase in the peak intensities upon increasing the gamma irradiation doses. The UV–Vis spectra demonstrate a decrease in transmittance, and the band gap of the TiO_2 thin films decreases with an increase in the gamma irradiation doses. The Nyquist plots reveal that the overall charge-transfer resistance increases upon increasing the gamma irradiation doses. The equivalent circuit, series resistance, contact resistance, and interface capacitance are measured by simulation using Z-view software. The present work demonstrates that gamma irradiation-induced defects play a major role in the modification of the structural, electrical, and optical properties of the TiO_2 thin films.

Keywords ALD · Gamma irradiation · Impedance spectroscopy · Optical band gap · Photoluminescence

1 Introduction

Among semiconducting oxides, TiO_2 has received much attention because of its chemical and physical properties such as non-toxicity, stability, wide band gap, high refractive index, permittivity, and high transmittance in the visible region [1, 2]. TiO_2 films have three different structural phases: anatase, rutile, and brookite [3–6]. Depending on the structural phase, TiO_2 has different applications such as gas sensors [7], optical cells [8], optical filters [9], solar energy conversion [10], antireflection coatings [11], waveguides [12], photocatalysts [13], and ceramic membranes [14]. TiO_2 is one of the most attractive materials for the window layer in solar cells [15]. For solar cell applications, the main requirement of a wide-gap semiconductor is high optical transmission. The optical electronic transport properties of TiO_2 strongly depend on the deposition methodology and the structural phase.

Several deposition techniques such as liquid-phase crystal deposition [16], sol–gel deposition [17, 18], hydrothermal deposition [19, 20], and electrophoretic deposition [21] have been used to deposit TiO_2 films. Atomic layer deposition (ALD) has significant advantages over the other methods, such as stoichiometric control, low-temperature processing, precision in material thickness, and self-limiting nature [22].

This work was supported by King Saud University, Deanship of Scientific Research, and College of Science Research Center.

✉ Syed Mansoor Ali
mansoor_phys@yahoo.com

[1] Department of Physics and Astronomy, College of Science, King Saud University, P.O. BOX 2455, Riyadh 11451, Saudi Arabia

[2] National Center for Irradiation Technology, King Abdulaziz City for Science and Technology, Riyadh, Saudi Arabia

[3] Department of Physics, COMSATS Institute of Information and Technology, Lahore, Pakistan

[4] Department of Physics, Faculty of Science, University of Gujrat, Hafiz Hayat Campus, Gujrat, Pakistan

Oxide semiconductors are highly responsive to gamma radiation. The gamma radiation dissipates as energy into the lattice of the material. In general, gamma radiation interacts with the material in two ways: defect creation and defect annihilation [23]. The number of defects created is more than the number of defects annihilated at higher gamma irradiation doses, and vice versa at lower doses [24, 25]. Interaction with radiations can alter the optical, nanostructural, and electrical properties of thin films [26]. In this work, TiO_2 thin films were deposited on a fluorine-doped tin oxide (FTO) glass substrate by the ALD method, and the modification of the structural, optical, and electrical properties caused by gamma irradiation was studied.

2 Experimental

The TiO_2 thin films were deposited on FTO substrates using the ALD technique. First, the FTO glass was cleaned by washing with (HCl + H_2O_2 + 6 DI) solution and drying under nitrogen (N_2) flow. The deposition process for the TiO_2 thin films involved alternate cycles. The precursors ($TiC1_4$ and deionized water) were carried into the reaction chamber alternately using N_2 as the carrier gas under a flow rate of 200 sccm and pressure of 9 hPa. After each precursor cycle, the residual unreacted reactant and the byproduct from the reaction chamber were purged by pure N_2 gas. The pulse width and the growth rate per cycle were measured to be 0.1 s and 0.4 Å, respectively. 100-nm-thick TiO_2 thin films were obtained by performing 2500 cycles.

For irradiation, the TiO_2 films were exposed to a ^{60}Co gamma source with a half-life of 5.2714 years, energy of 1.25 MeV, and dose rate of 7.328 kGy/h; the dose was varied between 25, 50, 75, and 100 kGy.

XRD analysis of the as-deposited and gamma-irradiated samples was performed by using an X-ray diffractometer (Bruker, D8 Discover) with Cu-Kα source radiation. UV–Vis reflectance and transmittance measurements were taken at room temperature using a UV–Vis spectrophotometer (JASCO–V 670) in the wavelength range 200–800 nm. The room-temperature photoluminescence (PL) of the non-irradiated and gamma-irradiated TiO_2 samples was determined upon excitation at 325 nm using a spectrofluorometer (FP-8200). The impedance spectra were measured by a KEITHLEY 4200 SCS system at room temperature, in air, under dark conditions.

3 Results and discussion

The XRD patterns of the non-irradiated and gamma-irradiated TiO_2 films are depicted in Fig. 1. It can be clearly seen that the XRD patterns of the TiO_2 thin films before and after irradiation have plans analogous to FTO, anatase, and rutile. The diffraction patterns agreed well with those of the anatase and rutile phases after removal of the FTO peaks. As the gamma irradiation dose increased, all the peaks became more distinct and shifted to a larger 2θ value. The increase in the peak intensity indicated that the TiO_2 thin films became highly crystalline as the gamma irradiation dose was increased. The shift in the peaks might be due to the strain produced by gamma irradiation.

The average crystallite size (D), microstrain (μ), and dislocation (δ) of the TiO_2 films are calculated on the basis of the XRD results, using formulas 1 [27], 2 [28], and 3 [29]:

$$D = \frac{0.94\lambda}{\beta \cos\theta}, \tag{1}$$

$$\mu = \frac{\beta \cos\theta}{4}, \tag{2}$$

$$\delta = \frac{1}{D^2}, \tag{3}$$

where λ (1.5406 Å) is the wavelength of the X-ray, θ (°) is the diffraction angle, and β is the full width at half maximum of the peak (radian).

The crystallite size of the films decreased (97–55.7 nm) and the microstrain increased as the gamma irradiation dose was changed from 0 to 100 kGy. The calculated results based on the XRD patterns are given in Table 1.

Figure 2 shows the UV–Vis spectra of the non-irradiated and gamma-irradiated TiO_2 samples on the FTO substrate. It can be seen that the as-deposited sample shows high transmittance in the visible region, but there is a sudden decrease in transmittance in the ultraviolet region due to the deep absorption. The surface roughness of the thin films had a significant effect, especially in the transparent zone. After gamma irradiation, the roughness of the TiO_2 thin films led to a decrease in the transmission as a function of the dose.

For crystalline materials, direct transitions are valid according to Tauc's relation [30]. Subsequently, for the present TiO_2 thin films, only the direct band gap energy was determined by the Tauc linearization (Fig. 3). The optical band gap was determined to be 3.31 eV for the as-deposited sample, and it increased to 3.38 eV with an increase in the gamma irradiation dose. This difference may be attributed to the decrease in the particle size or oxygen defect band states formed in the band gap.

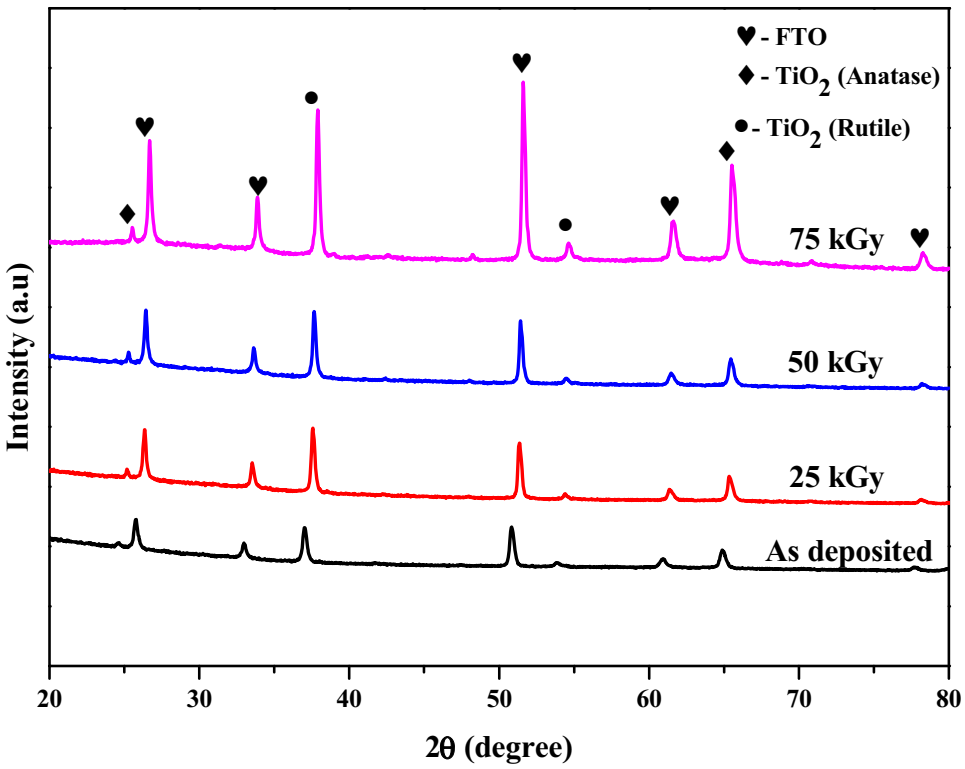

Fig. 1 (Color online) XRD patterns of TiO_2/FTO for different gamma irradiation doses

Table 1 Nanostructural parameters and energy band gap of TiO_2 thin films on FTO glass

Gamma irradiation dose	Crystallite size 'D' (Å)	Microstrain '$\mu \times 10^{-2}$'	Dislocation '$\delta \times 10^{18}$' (lines/m^2)	Band gap 'E_g' (eV)
As-deposited	9.70	6.3	1.6	3.31
25 kGy	5.86	6.7	3.34	3.34
50 kGy	5.63	6.9	2.25	3.36
75 kGy	5.57	6.94	3.61	3.38

Figure 4 depicts the PL spectra of the non-irradiated and gamma-irradiated TiO_2 thin films for different irradiation doses. It is clear that the gamma-irradiated TiO_2 films at three different excitation wavelengths (367, 378, and 550 nm) and the as-deposited sample show only one excitation (367 nm) [inset of Fig. 4]. The main excitation at 367 nm was due to the energy band gap emission for the non-irradiated and gamma-irradiated films. Since, the band gaps for the non-irradiated and irradiated samples were calculated from 3.31 to 3.38 eV. The emissions at 378 and 550 nm were lower than the band gaps of the films, implying that the gamma irradiation resulted in additional defect states within the band gap of the TiO_2 films. The intensity of the band gap and defect emission peaks clearly increased with an increase in the gamma irradiation dose, and the peaks shifted to the longer-wavelength side. The increase in the intensity of the emission peaks of the TiO_2 film strongly depended on the nanocrystalline structure. The traps in the band gap were probably associated with the intrinsic defects in the TiO_2 films. The XRD results for the TiO_2 thin films are favorable for the band gap emission (PL peak).

Frequency-dependent electrical conductivity measurements were taken for the as-deposited and gamma-irradiated TiO_2/FTO samples for the charge-transfer and recombination processes. As per the Nyquist plots shown

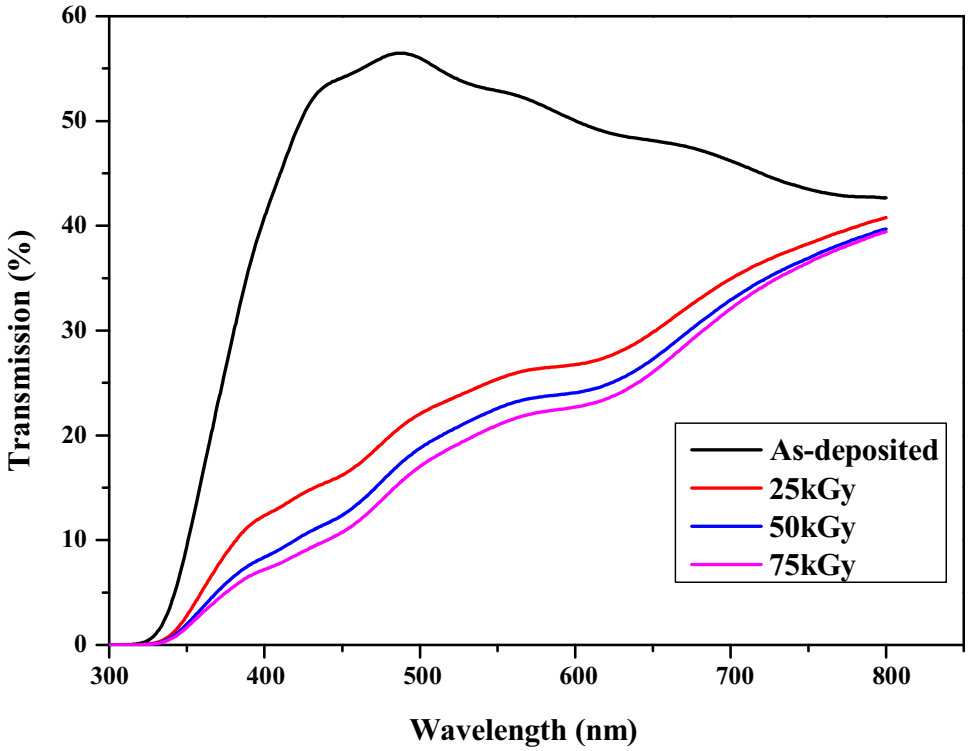

Fig. 2 (Color online) Transmission spectra of non-irradiated and gamma-irradiated TiO_2 thin films

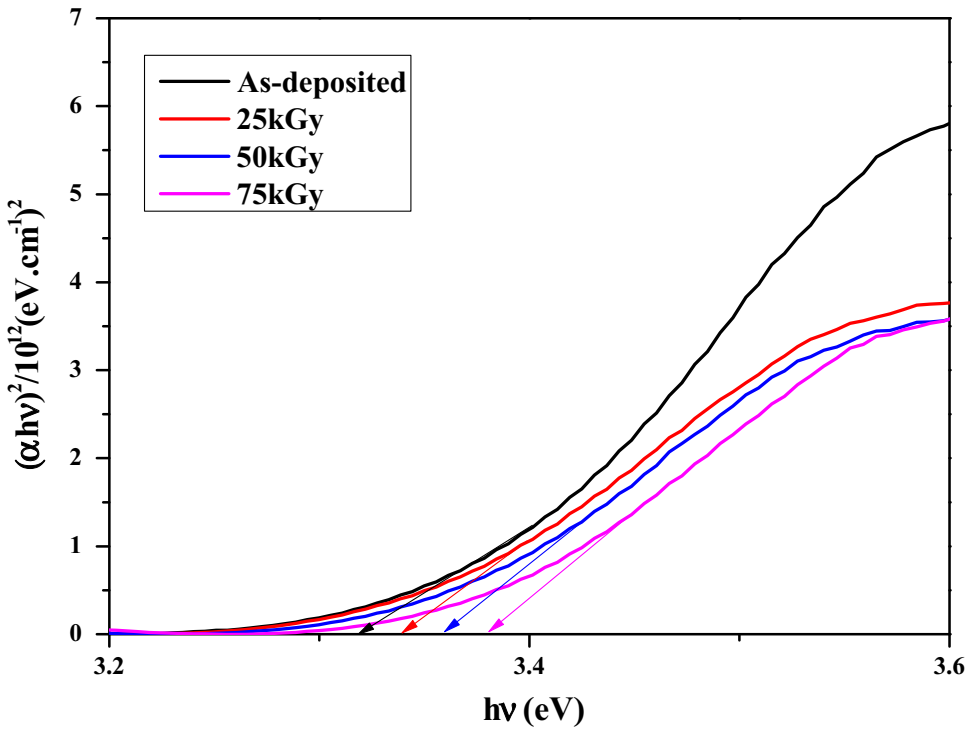

Fig. 3 (Color online) Tauc's plot for non-irradiated and gamma-irradiated TiO_2 thin films

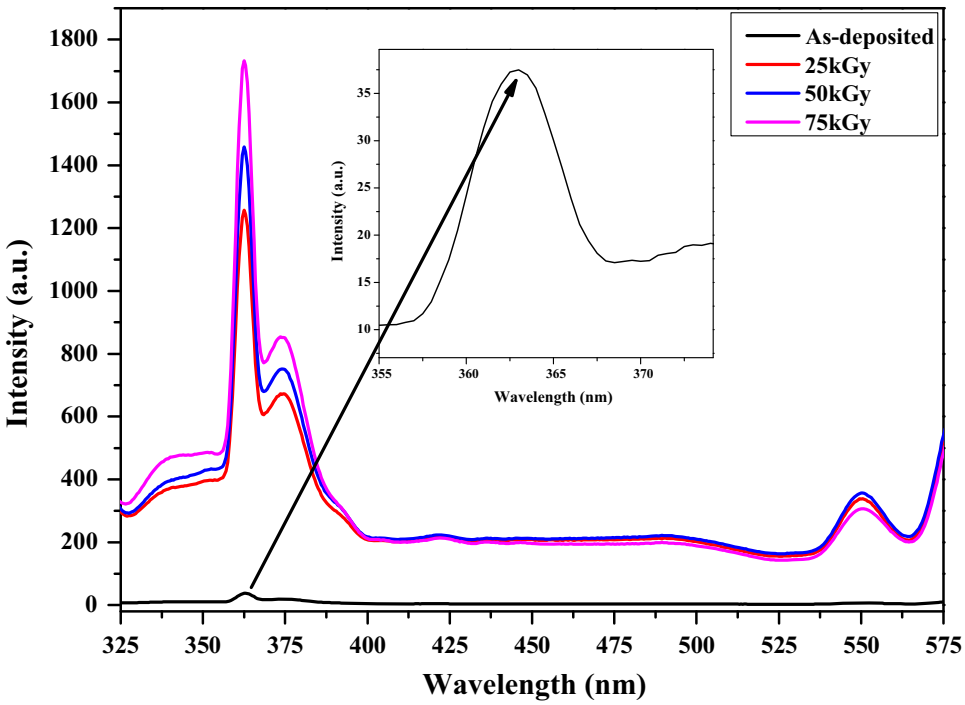

Fig. 4 (Color online) Photoluminescence spectra of non-irradiated and gamma-irradiated TiO_2 thin films

in Fig. 5a–d, each sample exhibits a semicircle in the low-frequency region, which is associated with the electron transport mechanism at the interface between TiO_2 and FTO. The electron transport resistance decreased with an increase in the gamma irradiation dose.

The semicircle fitting of the non-irradiated and gamma-irradiated TiO_2 thin films represents a single charge transportation process. The equivalent circuit obtained by the simulation of the experimental data can be seen in Fig. 6a, where R_s indicates the contact resistance, $R_{TiO2|FTO}$ indicates the bulk resistance of the films, and C_p denotes the interface capacitance. The simulated values of all these parameters are obtained using Z-View software and listed in Table 2.

The Bode and phase angle diagrams of the non-irradiated and gamma-irradiated TiO_2 thin films are shown in Fig. 6b. As the peak frequency of the middle semicircle has an inverse relationship with the electron lifetime at the TiO_2/FTO interface, the peak frequency increases, indicating a decrease in the lifetime with increased gamma irradiation doses.

4 Conclusion

We investigated the gamma irradiation-induced modification effects on the structure optical and electrical properties of TiO_2 films deposited by ALD. The XRD results for the irradiated TiO_2 films revealed an enhancement of the crystallinity. The microstrain and crystallite size increased upon increasing the gamma irradiation dose. The energy band gap and refractive index of the TiO_2 films, as determined by UV–Vis spectroscopy, increased for the initial dose and then decreased with increasing doses. The two extra peaks after irradiation could be due to the electron captured by the surface defects and the traps produced by the oxygen deficiencies. In the Nyquist plots for each sample, a semicircle appeared in the low-frequency region, which was associated with the charge-transfer process at the TiO_2/FTO interface. The charge-transfer resistance decreased with increasing gamma irradiation doses. The electron lifetime of the samples, which was calculated from the Bode phase plot, decreased upon increasing the gamma irradiation doses.

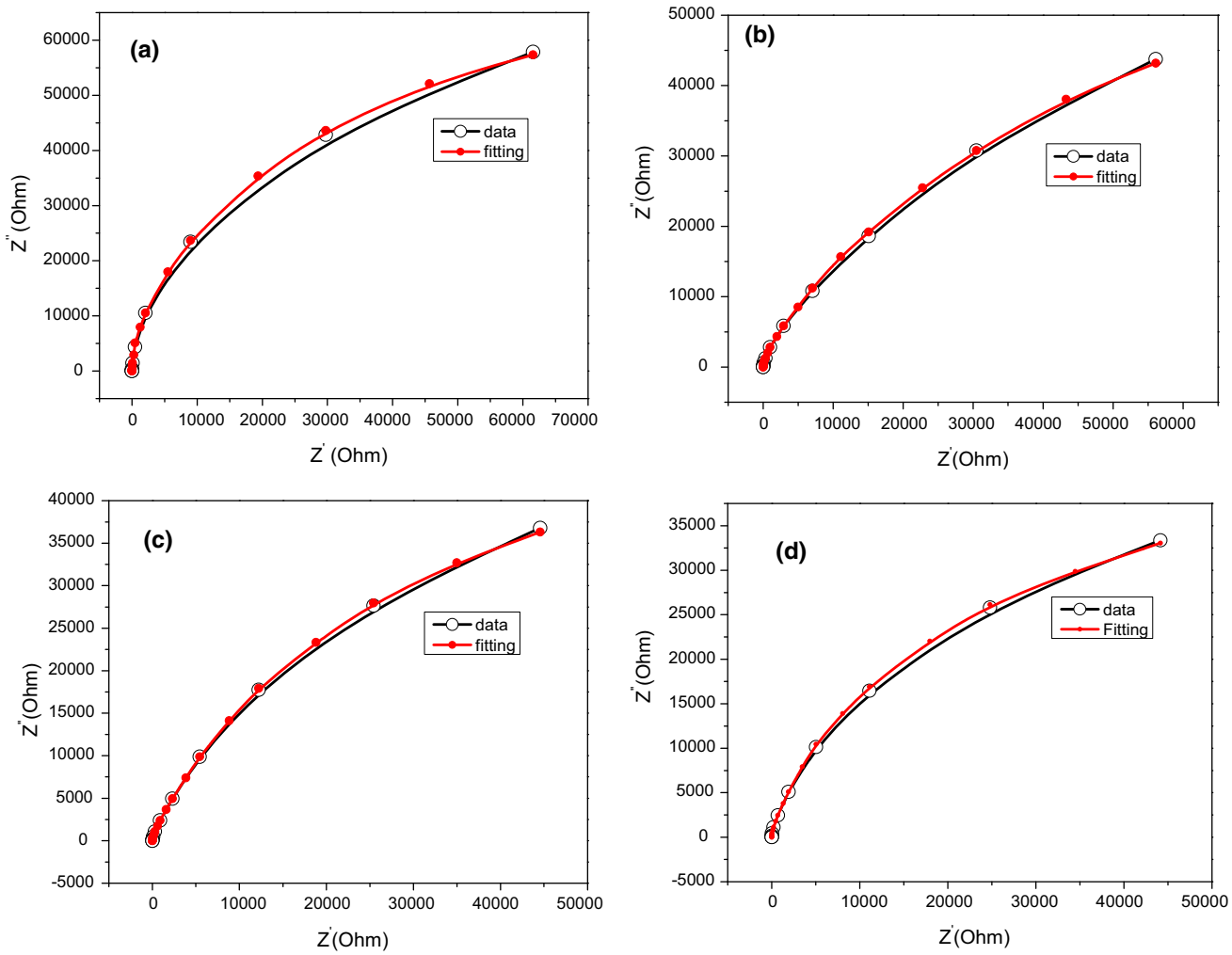

Fig. 5 (Color online) Nyquist plots for non-irradiated and gamma-irradiated TiO_2 thin films

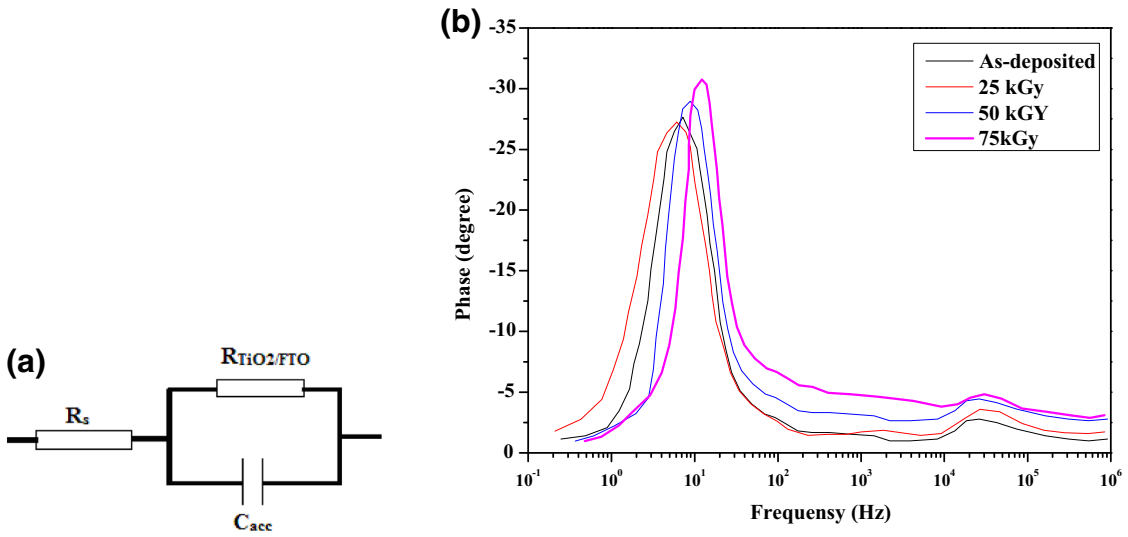

Fig. 6 (Color online) **a** Equivalent circuit and **b** Bode plot of non-irradiated and gamma-irradiated TiO_2 thin films

Table 2 Impedance results for TiO_2 thin films on FTO glass

Gamma irradiation dose	R_s (ohm × 10^3)	$R_{TiO2/FTO}$ (ohm × 10^9)	C_p (F × 10^{12})
As-deposited	6.5	1.2	1.3
25 kGy	6.9	0.7	1.3
50 kGy	7.5	1.9	1.3
75 kGy	8.5	1.2	1.3

References

1. S. Konstantinidis, J.P. Dauchot, M. Hecq, Titanium oxide thin films deposited by high-power impulse magnetron sputtering. Thin Solid Films **515**, 1182 (2006). https://doi.org/10.1016/j.tsf.2006.07.089
2. A. Mills, S.L. Hunte, An overview of semiconductor photocatalysis. J. Photochem. Photobiol. A Chem. **108**, 1 (1997). https://doi.org/10.1016/S1010-6030(97)00118-4
3. Z. Wang, U. Helmersson, P. Kall, Optical properties of anatase TiO_2 thin films prepared by aqueous sol–gel process at low temperature. J. Thin Solid Films **405**, 50 (2002). https://doi.org/10.1016/S0040-6090(01)01767-9
4. S. Richardon, A. Thruston, T. Collette, Identification of TiO_2/UV disinfection byproducts in drinking water. J. Environ. Sci. Technol. **30**, 3327 (1996). https://doi.org/10.1021/es960142m
5. R. Zhang, L. Gao, Q. Zhang, Photodegradation of surfactants on the nanosized TiO_2 prepared by hydrolysis of the alkoxide titanium. J. Chemosphere **54**, 405 (2004). https://doi.org/10.1016/S0045-6535(03)00588-5
6. D.G. Shchukin, D.V. Sviridov, Photocatalytic processes in spatially confined micro- and nanoreactors. J. Photochem. Photobiol. C **7**, 23 (2006). https://doi.org/10.1016/j.jphotochemrev.2006.03.002
7. H. Tang, K. Prasad, R. Sanjines, TiO_2 anatase thin films as gas sensors. Sens. Actuators B **71**, 26 (1995). https://doi.org/10.1016/0925-4005(94)01559-Z
8. B.E. Yoldas, T.W. O'keefee, Antireflective coatings applied from metal–organic derived liquid precursors. J. Appl. Opt. **18**, 3133 (1979). https://doi.org/10.1364/AO.18.003133
9. H. Kostlin, G. Frank, G. Hebbinghaus, Optical filters on linear halogen-lamps prepared by dip-coating. J. NonCryst. Solids **218**, 347 (1997). https://doi.org/10.1016/S0022-3093(97)00169-5
10. M.A. Butler, D.S. Ginley, Principles of photoelectrochemical solar energy conversion. J. Mater. Sci. **15**, 1 (1980). https://doi.org/10.1007/BF00552421
11. K. Bange, C.R. Ottermann, O. Anderson, Investigations of TiO_2 films deposited by different techniques. Thin Solid Films **197**, 279 (1991). https://doi.org/10.1016/0040-6090(91)90238-S
12. J. Zhai, T. Yang, L. Zhang, The optical waveguiding properties of TiO_2–SiO_2 composite films prepared by the sol–gel process. Ceram. Int. **25**, 667 (1999). https://doi.org/10.1016/S0272-8842(98)00081-9
13. J. Yu, X. Zhao, Q. Zhao, Photocatalytic activity of nanometer TiO_2 thin films prepared by the sol–gel method. Mater. Chem. Phys. **69**, 25 (2001). https://doi.org/10.1016/S0254-0584(00)00291-1
14. Y. Yan, S.R. Chaudhari, A. Sarkar, Synthesis, characterizations, and optical properties of stacked porous thin films derived from sol–gel process. J. Am. Ceram. Soc. **1996**, 79 (1061). https://doi.org/10.1111/j.1151-2916.1996.tb08548.x
15. Y. Chen, E. Stathatos, D.D. Dionysioua, Sol–gel modified TiO_2 powder films for high performance dye-sensitized solar cells. J. Photochem. Photobiol. A Chem. **203**, 192 (2009). https://doi.org/10.1016/j.jphotochem.2009.01.019
16. L.H. Kao, T.C. Hsu, H.Y. Lu, Sol-gel synthesis and morphological control of nanocrystalline TiO_2 via urea treatment. J. Colloid Interface Sci. **316**, 160 (2007). https://doi.org/10.1016/j.jcis.2007.07.062
17. M. Grätzel, Conversion of sunlight to electric power by nanocrystalline dye-sensitized solar cells. J. Photochem. Photobiol. A Chem. **164**, 3 (2004). https://doi.org/10.1016/j.jphotochem.2004.02.023
18. D. Wanga, B. Yua, F. Zhoua, et al., Synthesis and characterization of anatase TiO_2 nanotubes and their use in dye-sensitized solar cells. Mater. Chem. Phys. **113**, 602 (2009). https://doi.org/10.1016/j.matchemphys.2008.08.011
19. H.Z. Abdullah, C.C. Sorrell, TiO_2 thick films by electrophoretic deposition. J. Aust. Soc. **44**(2), 12 (2008)
20. J. Manríquez, L.A. Godínez, Tuning the structural, electrical and optical properties of Ti(III)-doped nanocrystalline TiO_2 films by electrophoretic deposition time. Thin Solid Films **515**, 3402 (2007). https://doi.org/10.1016/j.tsf.2006.09.055
21. N.P. Dasgupta, C. Liu, S. Andrews et al., Atomic layer deposition of platinum catalysts on nanowire surfaces for photoelectrochemical water reduction. J. Am. Chem. Soc. **135**, 12932 (2013). https://doi.org/10.1021/ja405680p
22. C. Clayeys, E. Simon, *Radiation Effect in Advanced Semiconductor Materials and Devices* (Springer, Berlin, 2002)
23. S.K. Khamari, V.K. Dixit, T. Ganguli et al., Effect of ^{60}Co gamma-ray irradiation on electrical properties of GaAs epilayer and GaAs p–i–n diode. Nucl. Inst. Methods Phys. Res. B **269**, 272 (2011). https://doi.org/10.1016/j.nimb.2010.11.067
24. E. Tanassova, A. Paskaleva, R. Konakova et al., Influence of γ-radiation on thin Ta_2O_5-Si structures. Microelectron. J. **32**, 553 (2001). https://doi.org/10.1016/S0026-2692(01)00043-X
25. M. Kumari, P. Rana, R.P. Chauhan, Modifications in structural and electrical properties of gamma irradiated CdSe nanowires. Nucl. Inst. Methods Phys. Res. A **753**, 116 (2014). https://doi.org/10.1016/j.nima.2014.03.062
26. C.S. Barret, T.B. Massalski, *Structure of Metals* (Pergamon Press, Oxford, 1980)
27. S.M. Ali, W.A. Farooq, M.R. Baig et al., Structural and optical properties of pure and Ag doped ZnO thin films obtained by sol gel spin coating technique. Mater. Sci. Pol. **33**(3), 601 (2015). https://doi.org/10.1515/msp-2015-0091
28. S. Rani, P. Suri, P.K. Shishodia et al., Synthesis of nanocrystalline ZnO powder via sol–gel route for dye-sensitized solar cells. Solar Energy Mater. Solar Cells **92**, 1639 (2008). https://doi.org/10.1016/j.solmat.2008.07.015
29. E.A. Davis, N.F. Mott, Conduction in non-crystalline systems V. Conductivity, optical absorption and photoconductivity in amorphous semiconductors. Philos. Mag. **22**, 903 (1970). https://doi.org/10.1080/14786437008221061
30. J. Tauc (ed.), *Amorphous and Liquid Semiconductors* (Plenum Press, London and New York, 1974)